Calculation of conduction-electron scattering rates from vacancies in copper and gold

A. J. Baratta* and A. Lodder
Natuurkundig Laboratorium, Vrije Universiteit, De Boelelaan 1081, 1081 HV Amsterdam, The Netherlands

D. E. Simanek
Physics Department, Lock Haven University, Lock Haven, Pennsylvania 17745
(Received 11 March 1987)

The impurity-cluster formalism has been applied to the question of conduction-electron scattering from vacancies in Cu and Au. Using self-consistent vacancy potentials in Cu and constructed potentials in Cu and Au, the Dingle temperatures for the ⟨111⟩ and ⟨100⟩ belly orbits and ⟨111⟩ neck orbit were calculated. Calculations were performed for both zero lattice distortion and distortion consistent with experimentally measured values. Comparison of the results shows that lattice distortion in the Au(vacancy) system must be included to predict correctly the observed anisotropy. For Cu with vacancies, the effect of lattice distortion is much smaller and may be neglected. The results show that the anisotropy of the scattering rate in Cu is due largely to charge redistribution around the vacancy. For Au, the anisotropy is produced by both the charge redistribution and the effects of the lattice distortion. The different behavior of the two materials was found to be due mainly to differences in their electronic structure rather than to the lattice distortion, which is comparable in the two metals.

I. INTRODUCTION

In the preceding paper,[1] we reported on vacancy-induced conduction-electron scattering in Cu. The results were obtained using magnetic-field-induced surface-state resonances to measure the point-by-point anisotropy of the scattering rate. We note in that paper that the anisotropy for the Cu(vacancy) system differed markedly from that for the Au(vacancy) system despite the fact that the two metals have similar Fermi surfaces and low-temperature lattice distortion. The purpose of this paper is to explore the reason for the differences in anisotropy and to determine the electronic structure of the vacancy.

The results given in the preceding paper[1] showed that the scattering rates and Dingle temperatures for the Cu(vacancy) system were highest for the neck and lower for the belly regions. For Au, Lengeler[2] found that the Dingle temperature and scattering rates were lowest for the neck and moderately higher for the belly regions. He also noted that when the vacancy potential was modeled as a constant potential within the muffin-tin approximation, the resulting neck Dingle temperatures were low by nearly a factor of 2 despite the fact that the model predicted belly temperatures in good agreement with the experimental data. Lengeler suggests that lattice relaxation not included in his model may have to be accounted for to predict correctly the scattering rates.

The approach used by Lengeler to calculate the scattering from a vacancy in Au is that due to Coleridge, Holzwarth, and Lee.[3–5] Using a generalized phase-shift analysis for the scattering of Bloch waves from defects in noble metals, quantities such as Dingle temperatures and changes in Fermi-surface cross-sectional areas may be calculated. The approach accounts for the scattering from the central potential as well as backscatter by the host lattice of the scattered wave. It has been used very successfully to describe a number of noble-metal alloys where lattice distortion is not too severe.[5] It breaks down, however, for cases in which the lattice distortion becomes large, such as Cu(Ge).

More recently, Lodder[6,7] has developed and Molenaar *et al.*[8,9] have applied to substitutional alloys a method which accounts for the relaxation of the nearest-neighbor atoms around an impurity defect. This formalism describes the scattering of Bloch electrons by a cluster, which consists of an impurity and the affected host atoms. Unlike the approach of Coleridge *et al.* changes in local environment such as charge transfer and lattice distortion can be accounted for.

In order to understand the effects of lattice distortion on vacancy-induced scattering, we have applied the cluster formulation to this problem. In the next section, the impurity cluster formalism is described. It is then applied to the Cu(vacancy) and Au(vacancy) system. The effects of lattice distortion on the scattering anisotropy in the two systems are examined and conclusions drawn in the final section. This section also includes a comparison with results for the Cu(vacancy) system obtained using a self-consistent potential by Braspenning *et al.*[10]

II. THE EFFECTS OF LATTICE DISTORTION ON SCATTERING RATES

A. Theory

The cluster T matrix contains all the information about the scattering of electrons from a defect cluster. The quantity is given by

$$T_{\mathbf{k}\mathbf{k}'}=\sum_{j,L,L'} C^{h\,*}_{\mathbf{k},jL}\,T^{j}_{LL'}\,C_{\mathbf{k}',jL'}\ , \tag{1}$$

where **k** denotes the wave vector and band index of the electron's Bloch state and L stands for the angular momentum-indices l and m. The host wave-function coefficients at the jth scatterer are given by

$$C^h_{k,jL}=\frac{-i^l E_F^{1/2} V_{L,0}}{\left[-\frac{\partial\lambda_0}{\partial E}\right]^{1/2}(\sin\eta_l^h)\exp(i\eta_l^h)}e^{i\mathbf{k}\cdot\mathbf{R}_j} . \quad (2)$$

Here $V_{L,0}$ and λ_0 are normalized eigenvectors and eigenvalues of the Korringa-Kohn-Rostoker (KKR) matrix. The subscript 0 denotes those eigenvectors and eigenvalues for which $\lambda_0(\mathbf{k},E_F)=0$. The quantities η_l^h are the host phase shifts. E_F is the Fermi energy.

According to KKR Green's-function theory, in the impurity cluster defect formalism[6–9] the alloy wave-function coefficients at the jth scatterer are related to the host wave-function coefficients $C_{k,jL}$ as

$$C_{k,jL}=\sum_{j',L'} A^{jj'}_{LL'}C^h_{k,j'L'} , \quad (3)$$

where the backscattering matrix $\underline{A}$ is given by

$$(\underline{A}^{-1})^{jj'}_{LL'}=J_{LL'}(-\Delta^j)\delta_{jj'}-\sum_{L''}G^{jj'}_{LL''}J_{L''L'}(-\Delta^{j'})(t^{j'}_{l'}-t^h_{l'}) . \quad (4)$$

The vector Δ is the difference between the actual position of the jth atom and its normal unperturbed position on a lattice site. $J_{LL'}(\Delta)$ is given by

$$J_{LL'}(\Delta)=4\pi i^{l-l'}\sum_{L''} i^{l''}C_{LL'L''}j_{l''}(E_F^{1/2}|\Delta|)Y_{L''}(\hat{\Delta}) . \quad (5)$$

It is this matrix which accounts for lattice distortion. Here $C_{LL'L''}$ is a Gaunt coefficient, j_l a spherical Bessel function, and Y_L a real spherical harmonic.

The local scattering information is contained in the t matrices

$$T^j_{LL'}=-E_F^{1/2}J_{LL'}(-\Delta^j)\sin(\eta^j_{l'}-\eta^h_l)\exp[i(\eta^j_{l'}-\eta^h_l)] \quad (6)$$

$$t^j_l=-E_F^{1/2}\sin\eta^j_l\exp(i\eta^j_l) , \quad (7)$$

where η^j_l are the phase shifts of an impurity cluster atom. Finally, the host Green's-function matrix $\underline{G}$ is determined by a Brillouin Zone integral involving the inverse of the KKR matrix.[11]

The typical parameters measured in experiments are the Dingle temperatures and the inverse relaxation times. These are related to the cluster t matrix by

$$\tau_k^{-1}=-2c\,\mathrm{Im}T_{kk} , \quad (8)$$

and

$$T_D=\frac{\hbar}{2\pi k_B}\langle\tau_k^{-1}\rangle_{\mathrm{orbit}} \quad (9)$$

B. Application

To investigate the effects of lattice distortion on the anisotropy of scattering rates and Dingle temperatures, a study of the Cu(vacancy) and Au(vacancy) systems was undertaken. To do so, a series of vacancy potentials were developed for both Cu and Au. In the case of Cu, a self-consistent potential for a vacancy in Cu was available from Braspenning and Zeller.[10,12] For Au, no such potential is available and *ab initio* potentials were used to derive the necessary phase shifts. This was also done for Cu to allow comparison with the results for Au. In addition, fitted phase shifts were available for Au(vacancy) and Cu(vacancy) systems.

The *ab initio* potentials were developed by starting with self-consistent relativistic atomic charge densities according to Desclaux.[13] The Mattheiss muffin-tin prescription was followed in computing the host and dilute-alloy potentials. The Fermi energy was fixed by the requirement that the volume inside the Fermi surface accommodate all conduction electrons. For noble metals, the number is 1 because the d electrons fill five Brillouin zones completely. If necessary, the impurity and first surrounding host-shell potentials were shifted by a constant potential in order to achieve charge neutrality as measured by the Friedel sum. Such a shift is interpreted as the amount of screening of the perturbed atoms.[14] The angular-momentum cutoff value for all sums was chosen as $l_{\max}=3$. In previous work by Molenaar[15] this cutoff was found necessary in order to account for both the d scattering and the influences of lattice distortion.

The self-consistent potentials of Braspenning and Zeller for Cu were obtained by starting from a self-consistent host potential by Moruzzi *et al.*[16] In the framework of the KKR Green's-function method a self-consistent single-site impurity potential was obtained and is indicated by SCP1 in the accompanying tables. Similarly, a self-consistent impurity cluster potential consisting of the impurity and 12 nearest neighbors, denoted by SCP13, was obtained by allowing the charge distribution of the nearest-neighbor atoms to relax around the vacancy. One should note that this relaxation accounts only for charge transfer and not for lattice distortion. It should also be noted that for these potentials, phase shifts were only available to $l_{\max}=2$.

Finally, for both Cu and Au, a set of fitted vacancy phase shifts were used, which resulted from a procedure in which the de Haas–van Alphen Fermi surface data and scattering rate data are fitted using single-site KKR Green's function expressions as discussed by Coleridge *et al.*[3] As in the self-consistent potentials, phase shifts were only available up to $l_{\max}=2$.

The phase shifts for each potential used as well as the host phase shifts, Fermi energies, and lattice constants are given in Table I. Table II contains the experimental and calculated Dingle temperatures obtained using the phase shifts in Table I, as well as the associated Friedel sums. In each case, the calculated Dingle temperatures are for zero lattice distortion.

For the Cu(vacancy) system the calculated Dingle temperatures obtained using the self-consistent potential

TABLE I. Values of phase shifts η_0, η_1, η_2, and η_3 in radians used in calculating the Dingle temperatures and scattering anisotropy for the various potentials discussed in the text. NSCP2 refers to the non-self-consistent potential where the constructed vacancy potential was shifted using a negative potential equal to 0.01 Ry and the nearest-neighbor Au atoms were shifted using a positive potential of 0.025 Ry.

Potential		η_0	η_1	η_2	η_3
		Cu(vacancy)			
SCP 13					
$E_F=0.63$ (Ry)	Host	−0.0957	0.0884	−0.1542	
$a_0=6.76$ (Å)	Vacancy	−0.7106	−0.1800	−0.0227	
	First shell	−0.1263	0.0722	−0.1617	
NSCP1					
$E_F=0.584$ (Ry)	Host	−0.044 997	0.095 483	−0.127 75	0.001 08
$a_0=6.830\,87$ (Å)	Vacancy	−0.472 269 9	−0.105 412	−0.012 629	−0.000 632
	First shell	−0.078 331	0.078 857	−0.135 76	0.000 922
Fitted					
$E_F=0.55$ (Ry)	Host	0.0755	0.1298	−0.1186	
$a_0=6.830\,87$ (Å)	Vacancy	0.9966	−0.5652	−0.1186	
		Au(vacancy)			
NSCP2					
$E_F=0.663$ (Ry)	Host	−0.412 87	−0.085 93	−0.301 82	0.007 368
$a_0=7.6821$ (Å)	Vacancy	−0.840 81	−0.261 94	−0.450 01	−0.004 025
	First shell	−0.455 379	−0.108 91	−0.316 84	0.006 685
Fitted					
$E_F=0.53$ (Ry)	Host	0.249 56	0.063 15	−0.2426	
$a_0=7.682\$\,115$ (Å)	Vacancy	−0.4748	−0.3459	−0.0278	

SCP13 and zero lattice distortion appear too high compared to experiment. They do exhibit the correct anisotropy with the two belly Dingle temperatures nearly equal and the neck higher by about 30%. Note nevertheless the impressive improvement in Friedel sum and Dingle temperatures in going from SCP1, the single-site potential, to SCP13. The constructed potentials appear to yield even better agreement with experiment than the self consistent potentials since both the ratios and Dingle temperatures are close to the experimental values.

By comparison, the Au(vacancy) calculation produces values for the Dingle temperatures that are low compared to the experiment. Also, the anisotropy is not reproduced very well at all by this calculation. One possible explanation of course is the fact that these calculations do not include lattice distortion.

To assess the impact of lattice distortion on the ratios, a series of calculations were performed in which the nearest neighbors, or 12 first-shell atoms were displaced inwards towards the vacancy. Figure 1 summarizes the results. Plotted are the ratios of ⟨111⟩ neck to ⟨100⟩ and ⟨111⟩ belly orbit Dingle temperatures for Au and Cu as a function of displacement. The displacements are in units of 0.01 times the lattice constants. If needed, the vacancy potential and first shell host potentials were shifted to maintain a Friedel sum of -1.00 ± 0.03.

It is seen that as the lattice distortion increases, the neck-to-belly ratios decrease for both Cu and Au. For

TABLE II. Comparison of calculated and experimental Dingle temperatures for ⟨111⟩ and ⟨100⟩ belly orbits (B) and ⟨111⟩ neck orbit (N) in Cu with vacancies and Au with vacancies. The first column denotes the potential. The second column gives the Friedel sum for each potential in electron units. Dingle temperatures are in units of 100 K/at.%. The last two columns give the neck-to-belly ratios. Dingle temperatures were calculated assuming zero lattice distortion.

			T_{D*}/C			
Potential	F	$B\langle 111\rangle$	$N\langle 111\rangle$	$B\langle 100\rangle$	$N\langle 111\rangle$:$B\langle 111\rangle$	$N\langle 111\rangle$:$B\langle 100\rangle$
			Cu(vacancy)			
SCP1	−0.7758	0.597	0.499	0.686	0.84	0.72
SCP13	−1.0480	0.279	0.361	0.288	1.3	1.3
NSCP1	−1.007	0.183	0.280	0.178	1.53	1.57
Experiment		0.175	0.275	0.189	1.6	1.5
			Au(vacancy)			
NSCP2	−1.006	0.228	0.306	0.208	1.34	1.47
Experiment		0.387	0.338	0.383	0.87	0.88

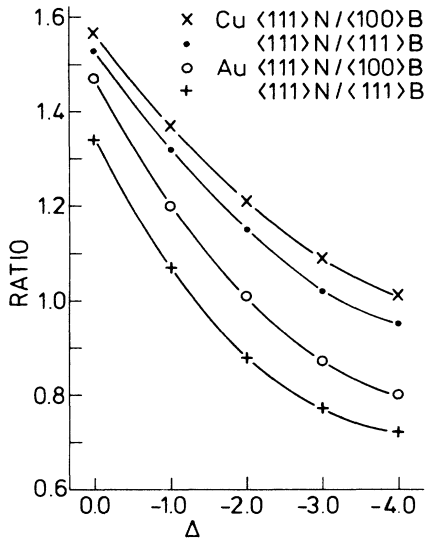

FIG. 1. Ratios of neck-to-belly Dingle temperatures in Cu and Au with vacancies as a function of displacement Δ of the nearest neighbors. The displacement is in units of 0.01 times the lattice constant.

Cu, the decrease is more gradual than for Au. In the case of Au, the ratio of ⟨111⟩ neck to ⟨111⟩ belly decreases by 34% when the lattice distortion is increased from 0.0 to −2.0. For Cu, the ratio decreases by 25%. A similar trend occurs for the ratio of ⟨111⟩ neck to ⟨100⟩ belly. The trend of the Dingle-temperature ratios as well as the more rapid decrease in Au ratios compared to Cu ratios was found to be independent of the potential shifts used. This suggests that the origin of the difference in vacancy scattering for the two noble metals is associated with the effect of lattice distortion rather than charge transfer.

III. COMPARISON WITH EXPERIMENTAL VALUES

To compare the calculated results in Fig. 1 with the experimental values in Table II, it is necessary to know the local lattice distortion.

Oppeneer[17] has shown that the Eshelby theory[18] can be used to develop estimates of the first-shell lattice distortion around an imperfection. If one obtains experimentally the macroscopic volume change $\Delta V/V$ then the relaxation of the nearest-neighbor, Δ, for a fcc material may be determined from

$$|\Delta| = \frac{1}{24\pi}\frac{1+\sigma}{1-\sigma}a\left|\frac{\Delta V}{V}\right|, \tag{10}$$

where σ is Poisson's ratio and a the lattice constant. Table III gives vacancy relaxation volumes from the literature as reported by Ehrhart *et al.*[19] Also given are the lattice relaxations Δ for Au and Cu using Eq. (10) and 0.423 and 0.350 for Poisson's ratio, respectively. From the Au data plotted in Figure 1, values of Δ around −1.8 yield a value of 0.9 for the ratio of ⟨111⟩ neck to ⟨111⟩ belly in Au and a value 1.03 for the ratio of ⟨111⟩ neck to ⟨100⟩ belly. These values are higher than the experimental ratios for Au given in Table II but within experimental uncertainty. Using a value of −0.6 for the lattice relaxation in Cu yield values of 1.4 for the ratio of ⟨111⟩ neck to ⟨111⟩ belly and 1.44 for the ratio of ⟨111⟩ neck to ⟨100⟩ belly. These results are somewhat lower than the experimental values of Table II. Nonetheless, these results do show that the lattice distortion in Au and Cu produce an inversion in the neck-to-belly ratios. The ratios are clearly larger for Cu and smaller for Au, consistent with experiment. This is true even if Ehrhart's smaller value of $\Delta V/V$ for Au is used. Although in that case the ratios are much greater than

TABLE III. Relaxation volumes reported in the literature for Cu and Au with vacancies and associated first-shell relaxation Δ in units of the lattice constant times 0.01. The quantity σ is Poisson's ratio.

	$\Delta V/V$	Δ
	Au	
$\sigma=0.423$	-0.44 ∓ 0.02[a]	−1.4
	−0.55[b]	−1.8
	−0.57[c]	−1.9
	-0.15 ∓ 0.06[d]	−0.69
	Cu	
$\sigma=0.350$	−0.2[e]	−0.6
	−0.3[f]	−0.83

[a]Reference 20.
[b]Reference 21.
[c]Reference 22.
[d]Reference 22,19.
[e]Reference 19,23.
[f]Reference 24.

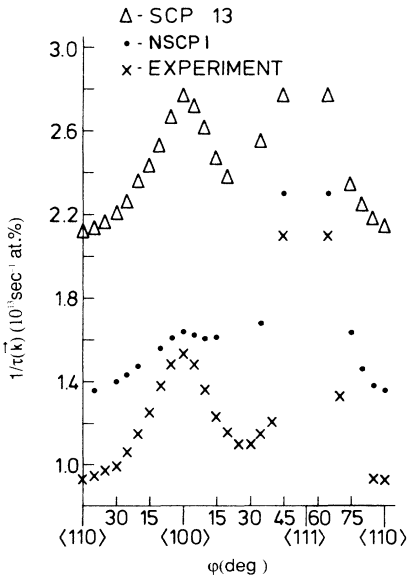

FIG. 2. Comparison of experimentally measured scattering rate anisotropy $1/\tau(\mathbf{k})$ from vacancies in Cu with that calculated using a self-consistent potential and a constructed potential.

the experimental values.

The discrepancy between the calculated Dingle temperatures and ratios and the experimental values is most likely due to the inadequacy of the potentials used in this study. To further evaluate the potentials, the point-by-point scattering rate in Cu with vacancies was calculated from Eq. (8) and compared with the results obtained using Friedel phase shifts which were fit to the actual experimental point-by-point scattering rates. The comparison was made in this way to allow the anisotropy of the scattering to be evaluated at points not measured experimentally.

Figure 2 compares the experimental anisotropy with the point by point scattering rate as determined using the self-consistent potential SCP13 and the non-self-consistent constructed potential denoted by NSCP1 where the constructed vacancy potential was shifted using a negative potential equal to 0.15 Ry and the nearest-neighbor Cu atoms were shifted using a positive potential of 0.007 Ry. The earlier discussion of the calculated Dingle temperature anisotropies suggested that the non-self-consistent potential gave results which compared more favorably with the experimental data. Figure 2, however, shows that the detailed anisotropy of the scattering rate is poorly reproduced by the non-self-consistent potential. By comparison the anisotropy calculated using the self-consistent potential agrees quite well with the experimental data. The better agreement is most likely due to a more accurate accounting of the radial charge redistribution at and around the vacancy in the self-consistent calculation than in the constructed potential calculation. As mentioned earlier, in the constructed potential, charge redistribution is approximated by somewhat arbitrary constant shifts of the vacancy and first-shell potentials.

It is also interesting to note that the self-consistent potential anisotropy gives better agreement despite the fact that the calculation for that case does not include lattice distortion. This suggests that the lattice distortion does not contribute significantly to the anisotropy of the scattering rate from a vacancy in Cu. To understand this aspect it is useful to examine more closely how the lattice distortion actually affects the scattering anisotropy.

Lattice distortion enters into the expression for the cluster t matrix through the transformation matrix $J_{LL'}$ [see Eqs. (4) and (6)].

An alternative way of expressing $J_{LL'}$ is

$$J_{LL'}(\Delta)=i^{l-l'}\int d\mathbf{k}\, Y_L(\mathbf{k})e^{i\mathbf{k}\cdot\Delta}Y_{L'}(\mathbf{k})\ . \tag{11}$$

One can easily show from this expression that for small lattice distortion, $J_{LL'}$ may be written to first order in the shifts Δ as

$$J_{LL'}=\delta_{LL'}+i^{l-l'+1}(\mathbf{k}\cdot\Delta)_{LL'}$$

with

$$(\mathbf{k}\cdot\Delta)_{LL'}=0 \quad \text{for } l\neq l'\pm 1\ .$$

The effect of lattice distortion on the backscattering renormalization matrix $\underline{A}$ [Eq. (4)] and the expression for the impurity t matrix [Eq. (6)] is to couple adjacent angular momentum states ($l=l'\pm 1$). The strength of the coupling is determined however not only by the magnitude of the lattice distortion but also by the difference between the phase shifts of the displaced atoms and the host atoms. Referring to Table I, one sees that the absolute difference in the phase shifts of the first shell and host for $l'=l\pm 1$ are not as great in Cu as they are in Au. Note particularly the difference when $l'=0$ or 2 and $l=1$. Thus one would expect that for the same lattice distortion the effect on the scattering anisotropy would be greater in Au than in Cu. This is in fact what is observed in Fig. 1. Thus we conclude that the difference in relative values of the phase shifts as well as the larger lattice distortion are needed to produce the anisotropy observed in Au compared to that observed in Cu. Further, we have shown that as postulated by Lengeler it is necessary to account for lattice distortion around a vacancy to predict correctly the Dingle temperatures anisotropy in Au.

ACKNOWLEDGMENTS

The authors thank Professor P. H. Dederichs, Dr. R. Zeller, and Mr. P. M. Oppeneer for helpful discussion and comments on this work. Particular thanks is extended to Dr. J. Molenaar for his efforts in assisting us with the calculations and Dr. A. C. Ehrlich for his helpful comments on the work and manuscript.

*Permanent address: The Pennsylvania State University, University Park, PA 16802.

[1]D. E. Simanek, A. J. Baratta, and A. Lodder, preceding paper, Phys. Rev. B **36**, 9082 (1987).
[2]B. Lengeler, Phys. Rev. B **15**, 5504 (1977).
[3]P. T. Coleridge, N A. W. Holzwarth, and M. J. G. Lee, Phys. Rev. B **10**, 1213 (1974).
[4]N. A. W. Holzwarth and M. J. G. Lee, Phys. Rev. B **13**, 2331 (1976).
[5]M. J. G. Lee, N. A. W. Holzwarth, and P. T. Coleridge, Phys. Rev. B **13**, 3249 (1976).
[6]A. Lodder, J. Phys. **6**, 1855 (1976).
[7]A. Lodder, J. Phys. F **7**, 139 (1976).
[8]J. Molenaar, A. Lodder, and P. T. Coleridge, J. Phys. F **13**, 839 (1983).
[9]J. Molenaar and A. Lodder, J. Phys. F **13**, 2063 (1983).
[10]P. J. Braspenning, R. Zeller, A. Lodder, and P. H. Dederichs, Phys. Rev. B **29**, 703 (1984).
[11]J. Molenaar, P. T. Coleridge, and A. Lodder, J. Phys. C **15**, 6955 (1982).
[12]R. Zeller and P. J. Braspenning, Solid State Commun. **42**, 701 (1982).
[13]J. P. Desclaux, Comput. Phys. Commun. **9**, 31 (1975).
[14]R. H. Lasseter and P. Soven, Phys. Rev. B **8**, 2416 (1973).
[15]J. Molenaar and A. Lodder, J. Phys. F **13**, 1501 (1983); **13**, 2205 (1983).

[16]V. L. Moruzzi, J. F. Janak, and A. R. Williams, *Calculated Properties of Metals* (Pergamon, New York, 1978).
[17]P. Oppeneer, Ph.D. thesis, Vrije Universiteit, Amsterdam, The Netherlands, 1987.
[18]J. D. Eshelby, J. Appl. Phys. **25**, 255 (1954).
[19]P. Ehrhart, H. D. Carstanjen, A. M. Fattah, and J. B. Roberto, Philos. Mag. A **40**, 843 (1979).
[20]W. Hertz, W. Waidelich, and H. Peisl, Phys. Lett. **43A**, 289 (1973).
[21]J. E. Bauerle and J. S. Koehler, Phys. Rev. **107**, 1493 (1957).
[22]J. Takamura, Acta Metall. **9**, 547 (1961).
[23]H. G. Haubold and D. Martinsen, J. Nucl. Mater. **69/70**, 644 (1978).
[24]P. Ehrhart and U. Schlagheck, J. Phys. F **4**, 1575 (1974).